Accumulation and retention of radioactive elements in biofilm communities surrounding the accident site of the Fukushima Daiichi Nuclear Power Plant

Shigeharu Moriya[1, 3, *], Hideaki Otsu[2], Kumiko Kihara[1, 4], Yukari Kato[1], Misao Itouga[1], Kenji Sakata[1], Jun Kikuchi[1, 3], Hiroshi Yamakawa[5, 6] and Jiro Suga[6]

1) RIKEN Center for Sustainable Resource Science, 1-7-22 Suehiro-cho, Tsurumi-ku, Yokohama city, Kanagawa 230-0045, JAPAN

Shigeharu Moriya, Kumiko Kihara, Yukari Kato, Misao Itouga, Kenji Sakata, and Jun Kikuchi

2) RIKEN Nishina Center for Accelerator-Based Science, 2-1 Hirosamwa, Wako city, Saitama 351-0198, JAPAN

Hideaki Otsu

3) Graduate School of Medical Life Science, Yokohama-city University, 1-7-29 Suehiro-cho, Tsurumi-ku, Yokohama city, Kanagawa 230-0045, JAPAN

Shigeharu Moriya and Jun Kikuchi

4) Department of Biological and Chemical Systems Engineering, National Institute of Technology, Kumamoto College, 2627 Hirayama-Shinmachi, Yatsushiro-shi, Kumamoto 866-8501, JAPAN

Kumiko Kihara

5) Tokyo University of Marine Science and Technology, 4-5-7 Konan, Minato-ku, Tokyo 108-8477, JAPAN

23 Hiroshi Yamakawa

24 6) Japan Academy of Underwater Sciences, 3-9-1-301 Botan, Koto-ku, Tokyo 135-0046,

25 JAPAN

26 Hiroshi Yamakawa and Jiro Suga

27

28 *Corresponding author: Shigeharu Moriya

29 RIKEN Center for Sustainable Resource Science, 1-7-22 Suehiro-cho, Tsurumi-ku,

30 Yokohama city, Kanagawa 230-0045, JAPAN

31 Tel +81-45-508-7221, Fax +81-45-508-7363

32 Email: smoriya@riken.jp

33

Abstract

After the Fukushima Daiichi Nuclear Power Plant accident, various surveys have been performed to measure the extent of radioactive contamination in marine sediments, surface waters, plankton, and fish. However, the radioactive contamination of one of the most important ecological niches, biofilms, has not been investigated. Therefore, in this study, we sampled biofilms from sea floor stones around Hisanohama Port, which is less than 30 km south of the accident site, and then analyzed the microbial community structure and element profiles, including those of radioactive elements, of these biofilms in order to determine the accumulation and retention of radioactive elements in them. Our results showed that the biofilm samples contained relatively high levels of radioactive cesium even when the sampling was performed 8–11 months after the accident. Our results also suggested that the structure of the biofilm organismal community is related to the element profile of radioactive cesium. Thus, our study suggests that biofilms are a possible radioactive compound accumulator in the natural environment and that they can retain radioactive material for at least 8–11 months.

Introduction

Following the Great East Japan Earthquake and catastrophic tsunami in March of 2011, the accident at the Fukushima Daiichi Nuclear Power Plant (FDNPP) led to the release of large amounts of radioactive materials into the atmosphere and marine environment. This release of radioactive elements from the FDNPP introduced a variety of radioisotopes,

56 especially radiocesium (^{134}Cs and ^{137}Cs), into marine waters. Public monitoring showed that
57 during several months after the first explosion at the FDNPP, a rapid decrease in
58 radioisotopes was observed in the nearby seawater. A joint official survey team from the
59 Tokyo Power Electric Company (TEPCO), Fukushima prefectural government, and the
60 Japanese Ministry of Education, Culture, Sports, Science and Technology (MEXT) reported
61 that the ^{137}Cs contamination level in the seawater quickly decreased from over 10 k Bq/L to
62 less than 100 Bq/L within a 2-month period. However, ^{137}Cs in the ocean sediments was
63 continuously observed over this period at levels between 100 Bq/dry kg and 1,000 Bq/dry kg
64 at least until September 2012 (Kanda, 2012). This disproportional distribution of
65 radioisotopes was also observed in marine fish by Wada et al., who reported that the
66 retention time of radiocesium appears to be remarkably longer in the larvae of demersal fish
67 such as *Sebastes cheni* than in surface fish such as *Eugraulis japonica* (Wada et al., 2013).
68 These disproportional distributions of radioactivity suggest that the sea floor eco-system,
69 including sedimental microbes and biofilms, may play role in the accumulation of
70 radioactive elements.
71 Therefore, in this study, we analyzed the biofilm community on the surface of sea floor rocks
72 with a focus on the element profiles, including those of radioactive elements. Our results
73 showed that all the biofilm community contained and retained relatively high levels of
74 radioactive cesium even when the sampling was performed 8–11 months after the accident.
75 Our findings indicate that biofilm organism community structures are likely related to their
76 element profiles, including that of radiocesium.
77

78

79 Materials and Methods

80 Sampling

81 Sampling was performed from November 11, 2011, to February 4, 2012. The sampling site
82 was the ocean along the coastline of Hisanohama, Iwaki City, Fukushima, Japan. We
83 collected samples 10 times within the established time period on November 11 (week 1),
84 November 20 (week 2), November 26 (week 3), December 3 (week 4), December 10 (week 5),
85 December 17 (week 6), January 14 (week 7), January 21 (week 8), January 29 (week 9), and
86 February 4 (week 10). Sampling was performed at six different locations near Hisanohama
87 Port: Area 1 (37.153762N 141.006167E, weeks 1 and 5), Area 2 (approximately 37.149863N
88 141.001017E, weeks 2, 8, and 9), Area 3 (approximately 37.146579N 141.002390E, week 4),
89 Area 3′ (approximately 37.147503N 141.008570E, week 10), Area 4 (approximately
90 37.133887N 141.002390E, weeks 3 and 7), and Area 4′ (approximately 37.142953N
91 141.003592E, week 6); all of these sampling sites are located 30 km south of the Fukushima
92 Nuclear Power Plant #1. Sampling was performed by divers using a self-contained
93 underwater breathing apparatus (SCUBA) at a depth of 5–10 m. The divers sampled the
94 bottom water and surface water (5 L) and collected bottom stones to obtain the biofilms. The
95 samplings were performed with permission from Fukushima Prefecture and the fishery
96 association of Iwaki City.

97

98 Sample preparation

99 The seawater samples were immediately filtered using two 24-mm-wide 0.22-μm Durapore

filters (Millipore, MA, USA) until they clogged. All the samples were then frozen at -20°C in a portable freezer prior to transportation back to the laboratory.

In the laboratory, the water samples were dried by boiling. The remaining salts (seawater salt) were allowed to settle into a U8 container, and the net weight (weight of container with sample – weight of empty container) and height of the samples were measured in the container.

In the case of biofilms, the bottom stones were rinsed with purified water and then brushed down with a clean brush using purified water. The obtained biofilm suspension was then divided into two aliquots. One aliquot was filtered through 24-mm-wide 0.22-μm Durapore filters (Millipore, MA, USA) and stored at -20°C for ribosomal RNA gene analysis, and the other one was dried at 105°C in an oven and then allowed to settle into a U8 container; the weight and height were then measured in the container for measurement of radioactivity.

Measurement of radioactivity

The gamma-ray activity of the samples in the containers was measured using a Germanium (Ge) detector. The detector setup was identical to that described previously (HABA et al., 2012). The energy resolution of 2 keV full width at half maximum (FWHM) was achieved at 1332.5 keV gamma rays. The sample location and detector were surrounded with 15-cm lead blocks to reduce the background radiation during gamma ray spectroscopy. The detection efficiency of the gamma rays was calibrated with an accuracy of 2%–10% using a multiple gamma ray standard source, which ranged from 88–1836 keV. A calibrated ^{134g}Cs source was also used to correct for the coincidence summing for radioactivity determinations of

^{134g}Cs.

Every sample was contained in a U8 plastic container. The U8 container is a standard container in Japan that is used for measurements of absolute radioactivity with high accuracy using a Ge detector. The shape of the container is cylindrical, with a diameter of 47 mm and height of 60 mm. The volume is approximately 100 mL. The efficiency calibration source is available within the container with a uniform density.

Every sample was measured using the Ge detector for at least 8 h to obtain sufficient statistics for each gamma ray peak. The relative geometry between the sample and the Ge detector was carefully reproduced by a guide apparatus at the sample location.

Gamma rays from ^{134}Cs and ^{137}Cs were observed for the biofilm samples. The radioactivity levels for every isotope were determined from the yield of the gamma rays corrected using the detection efficiency of the Ge detector and a geometrical acceptance between the sample and the detector. The geometric difference in the height of the sample from the calibration source was simulated using several electromagnetic simulation codes, including Geant4 (Agostinelli et al., 2003; Allison et al., 2006) and EGS5 (Hirayama et al., 2005). The radioactivity of the samples were normalized by weight.

Element analysis

To quantitatively analyze the content of 37 elements (^{7}Li, ^{9}Be, ^{23}Na, ^{24}Mg, ^{27}Al, ^{39}K, ^{43}Ca, ^{45}Sc, ^{47}Ti, ^{51}V, ^{52}Cr, ^{55}Mn, ^{57}Fe, ^{59}Co, ^{60}Ni, ^{63}Cu, ^{66}Zn, ^{85}Rb, ^{88}Sr, ^{98}Mo, ^{111}Cd, ^{133}Cs, ^{139}La, ^{140}Ce, ^{141}Pr, ^{146}Nd, ^{152}Sm, ^{153}Eu, ^{158}Gd, ^{159}Tb, ^{164}Dy, ^{165}Ho, ^{166}Er, ^{169}Tm, ^{172}Yb, ^{175}Lu, and ^{202}Hg) in the biofilm samples for measurement of radioactivity, the samples were predigested with 5

144 mL of concentrated HNO_3 for 1 h at room temperature. Next, the organic components were
145 completely decomposed by wet-ashing using a microwave sample preparation system
146 (Multi-Wave-3000, Perkin Elmer, MA USA) (Itouga et al., 2014). The digested samples were
147 then brought up to a volume of 50 mL using MilliQ water (MQW) and filtered through 5B
148 filter paper (Advantec, Tokyo, Japan). The concentrations of the mineral elements were
149 determined by Inductively Coupled Plasma Mass Spectrometry (ICP-MS, NexION300,
150 Perkin Elmer). For the ICP-MS analysis, a portion of the filtrated samples was diluted
151 appropriately with 0.01 mol/L HCl (Itouga et al., 2014). The mineral nutrient concentration
152 in the samples was calculated as a unit (mg/g in dry weight).
153 The obtained ICP-MS data were then normalized using the root-sum-of-squares (RSS) levels
154 for each element. Count data of radioactive cesium (^{134}Cs and ^{137}Cs) were treated with the
155 same calculation for normalization and then merged with the normalized ICP-MS dataset
156 (element table).
157
158 ssrDNA analysis
159 Genomic DNA was prepared from the stored biofilm samples by capturing on a 0.22-μm
160 Durapore filter, followed by bead-beating with phenol:chloroform:isoamyl alcohol (PCI)
161 extraction. Bead-beating was performed at 3000 rpm for 5 min (Micro Smash MS-100R,
162 TOMY, Tokyo, Japan), and nucleic acids were then recovered by ethanol precipitation.
163 PCR amplification was performed with the extracted genomic DNA using two primer sets
164 for 16S ssrDNA, 515F/806R (Caporaso et al., 2012; Caporaso et al., 2011) and 18S ssrDNA,
165 TAReuk454FWD1/TAReukREV3 (Stoeck et al., 2010). The primers were modified for

Illumina sequencing with a multi-index kit for the Nextera XT sequencing library construction kit (Illumina, CA, USA). We also added a "read1" sequence (5′- TCG GCA GCG TCA GAT GTG TAT AAG AGA CAG -3′) to the forward primers and a "read2" sequence (5′- GTC TCG TGG GCT CGG AGA TGT GTA TAA GAG ACA G -3′) to the reverse primers. PCR was performed with a standard reaction of ExTaq DNA polymerase according to the manufacturer's instructions (Takara Bio, Kyoto Japan) with 25 pmol of each primer/50 μL reaction mixture. The reactions were performed in a two-step PCR (10 cycles of 94°C for 30 s, 55°C for 45 s, and 72°C for 60 s, followed by 20 cycles of 94°C for 30 s and 72°C for 60 s) for 16S and a 3-step PCR (30 cycles of 94°C for 30 s, 55°C for 45 s and 72°C for 60 s) for 18S. The amplified products were then purified via 1% agarose gel electrophoresis. The obtained amplified products were applied to the NexteraXT (Illumina CA USA) sequencing library construction process without the "tagmentation" process.

A multi-index sequencing library was applied to the MiSeq sequencing kit v1 and read using Illumina MiSeq according to the instructions in the paired-end sequencing mode. Data were treated with MiSeq reporter software, and the reads were obtained from individual samples. After the extraction of the reads, the reads from weeks 4, 5, and 8 for the 18S ssrDNA were found to be insufficient for analysis. Therefore, subsequent analyses were performed using the reads from weeks 1, 2, 3, 6, 7, 9, and 10.

The obtained read data were then mapped onto the ribosomal RNA sequence library SILVA release 108 with the program package QIIME (Caporaso et al., 2010) using "Prefix-suffix operational taxonomy unit (OTU) picking," and the absolute abundance OTU table at the family level was constructed. Count zero data were manually removed from the table, and

188 the relative abundance values were calculated. The 16S and 18S data were treated
189 independently and then merged into a single OTU table with the relative abundance values.
190 Sequence data have been deposited in the DDBJ sequence read archive under the accession
191 number DRA004367.
192
193 Statistical analysis
194 For the statistical analysis, we used the program package R (R Core Team, 2014). First, we
195 drew a heatmap chart with hierarchical cluster analysis (HCA). The heatmap.3 function in
196 the GMD package, which is a package for non-parametric distance measurements between
197 two discrete frequency distributions (Zhao et al., 2011), was used to draw the heatmap with
198 HCA. Independent heatmaps were drawn from each element table and the OTU table with a
199 two-axis HCA. A scaling option was used for the OTU table treatment according to the row
200 direction but not for the elements table treatment.
201 Principal components analysis (PCA) was performed with the merged dataset, including
202 both the OTU table and elements table, using the prcomp function in R. Score plots were
203 drawn with principal component 1 (PC1; x-axis) and PC2 (y-axis). The loading plots for
204 quadrants II and III were drawn manually.
205
206
207 Results and Discussion
208 The gamma-ray energy spectra revealed significant peaks corresponding to natural
209 radioisotope signals, such as that of ^{40}K (data not shown), for all samples. Furthermore, we

found significant peaks corresponding to ^{134}Cs and ^{137}Cs from the biofilm samples. However, we did not detect signals for ^{134}Cs and ^{137}Cs from the sea water salts and particles captured on filter (Table 1).

Table 1. Peak detection from samples

	Peak detection	
Material	134Cs	137Cs
Surface sea water salt	−	−
Bottom sea water salt	−	−
Captured particles in surface water	−	−
Captured particles in bottom water	−	−
Biofilms on bottom rocks	+	+

+: significant peak detected from samples

−: significant peak not detected from all samples

Captured particles were filtered from water by 0.22um filter and measure radioactivity

It is possible that the ^{134}Cs (half-life: 2.0652 years) and ^{137}Cs (half-life: 30.1 years) released owing to prior nuclear weapons tests in the Pacific Ocean and the Chernobyl disaster have remained in the seabed around Japan. Therefore, we also analyzed samples collected from near Nishi-kawana in the Tokyo Bay (which is approximately 280 kilometers from the FDNPP) as controls, but found no significant signals for the radioisotopes ^{134}Cs and ^{137}Cs from these control samples. Therefore, we concluded that the radioisotopes detected in the samples around Hisanohama port in this study originated from the FDNPP disaster rather than from the environmental background or from past nuclear weapons tests. These results indicated that the biofilms on the sea floor around Hisanohama retained radioactive material for at least 8–11 months after the FDNPP accident.

However, the observed radioactivity level was different among the different biofilm samples

224 (Table 2). Therefore, we analyzed the relationship between the microbial consortia within
225 the biofilms and the elemental composition of the biofilms. To perform this analysis,
226 quantified element data were combined with radioactivity data for radiocesium (^{134}Cs and
227 ^{137}Cs) and utilized for statistical analysis. Ribosomal RNA genes were sequenced and used
228 to construct a dataset for the statistical analysis.

Table 2. Radioactivity of biofilm samples

		Cs134 Bq/kg dry	Cs137 Bq/kg dry
Week1	Area1	1141.78	1655.17
Week2	Area2	671.01	932.18
Week3	Area4	306.90	429.21
Week4	Area3	429.21	2353.58
Week5	Area1	926.40	1436.73
Week6	Area4'	538.56	829.08
Week7	Area4	844.49	1543.05
Week8	Area2	818.66	1607.65
Week9	Area2	359.77	591.46
Week10	Area3'	190.29	294.20

229 A HCA heat map chart from the dataset of elements and radiocesium (Fig. 1) showed
230 relatively higher content of radiocesium, Cr, Ni, Sc, Rb, Li, and cesium (Cs cluster) for the
231 week 1 sample than for other samples. Another remarkable profile from the elemental
232 analysis was observed in the week 3 sample, where high relative amounts of lanthanide
233 elements were detected (Lanth cluster).
234 A PCA score plot (Fig. 2A) of the merged dataset between the elements/radiocesium and the
235 microbial consortia showed that the week 1 sample was placed in the PC1 negative-PC2
236 positive direction, and the week 3 sample was placed in the PC1 negative-PC2 negative
237 direction. As mentioned above, the week 1 sample contained high relative amounts of Cs

cluster signals, and the week 3 sample contained high relative amounts of the Lanth cluster signals. Consistent with these findings, the PCA loading plot showed that the Cs cluster was placed in the PC1 negative-PC2 positive direction (Fig. 2B upper panel, Table S1), and the lanthanide cluster was placed in the PC1 negative-PC2 negative direction (Fig. 2B lower panel, Table S2). The results of the HCA heat map chart and PCA suggested that a "cesium-philic" biofilm occurred at the sampling point in the week 1 sample, and a "lanthanide-philic" biofilm occurred at the sampling point in the week 3 sample.

The PCA results from the datasets of both the elements and the microbes showed candidate organisms in the "cesium-philic" and "lanthanide-philic" biofilms on the loading plots, because those plots were placed in same loading direction, e.g., PC1 negative-PC2 positive (Cs cluster included) or PC1 negative-PC2 negative (Lanth cluster included, Fig. 2C, Table S1 and S2). Indeed, the HCA heat map of the organismal consortia showed that the PC1 negative-PC2 negative–directed organisms mainly appeared in the week 1 column (Fig. 3 blue dots). The same tendency was observed with the Lanth cluster organisms (Fig. 3 green dots). These results suggested that these two OTU sets are positively correlated with the Lanth cluster (week 3 sample) and Cs cluster (week 1 sample) elements.

Table 3. Cs cluster taxon in Week1 sample

OTU ID	Taxon information	Relative intensity
Primer18 S_Euk_2	Eukaryota;Alveolata;Dinophyceae;Gonyaulacales;Gonyaulacaceae	0.02974
Primer18 S_Euk_4	Eukaryota;Metazoa;Annelida;Clitellata;Oligochaeta	0.10316
Primer18	Eukaryota;Metazoa;Annelida;Polychaeta;Scolecida	0.02144

S_Euk_7		
Primer18		
S_Euk_8	Eukaryota;Metazoa;Arthropoda;Chelicerata;Arachnida	0.00847
Primer18		
S_Euk_11	Eukaryota;Metazoa;Arthropoda;Crustacea;Maxillopoda	0.06880
Primer18		
S_Euk_12	Eukaryota;Metazoa;Brachiopoda;Linguliformea;Lingulata	0.03599
Primer18		
S_Euk_15	Eukaryota;Metazoa;Cnidaria;Anthozoa;Hexacorallia	0.14012
Primer18		
S_Euk_23	Eukaryota;Metazoa;environmental samples;uncultured metazoan;Other	0.02215
Primer18		
S_Euk_25	Eukaryota;Rhodophyta;Florideophyceae;Ceramiales;Ceramiaceae	0.05550
Primer18		
S_Euk_27	Eukaryota;Rhodophyta;Florideophyceae;Ceramiales;Delesseriaceae	0.01796
Primer18		
S_Euk_34	Eukaryota;environmental samples;uncultured eukaryote;Other;Other	0.03092
Primer18	Eukaryota;environmental samples;uncultured freshwater	
S_Euk_35	eukaryote;Other;Other	0.00399
Primer18		
S_Euk_39	Eukaryota;stramenopiles;Chrysophyceae;Hibberdiales;Hibberdiaceae	0.00977
Primer16		
S_Arch_1	Archaea;Crenarchaeota;Marine Group I;uncultured archaeon;Other	0.06712
Primer16		
S_Bac_1	Bacteria;Acidobacteria;RB25;uncultured bacterium;Other	0.00588
Primer16	Bacteria;Actinobacteria;Acidimicrobiia;Acidimicrobiales;Sva0996 marine	
S_Bac_2	group	0.02444
Primer16		
S_Bac_3	Bacteria;Actinobacteria;Acidimicrobiia;Acidimicrobiales;uncultured	0.02674
Primer16		
S_Bac_4	Bacteria;Bacteroidetes;Cytophagia;Cytophagales;Flammeovirgaceae	0.07348
Primer16	Bacteria;Bacteroidetes;Flavobacteria;Flavobacteriales;Cryomorphaceae	0.00429

S_Bac_5		
Primer16	Bacteria;Bacteroidetes;Sphingobacteria;Sphingobacteriales;Saprospiracea	
S_Bac_7	e	0.01855
Primer16		
S_Bac_9	Bacteria;Cyanobacteria;Chloroplast;uncultured bacterium;Other	0.00919
Primer16	Bacteria;Proteobacteria;Alphaproteobacteria;Rhizobiales;Hyphomicrobiace	
S_Bac_16	ae	0.00994
Primer16	Bacteria;Proteobacteria;Alphaproteobacteria;Rhizobiales;Phyllobacteriace	
S_Bac_18	ae	0.00703
Primer16	Bacteria;Proteobacteria;Alphaproteobacteria;Rhodobacterales;Rhodobacte	
S_Bac_20	raceae	0.15535
Primer16	Bacteria;Proteobacteria;Alphaproteobacteria;Sphingomonadales;Erythroba	
S_Bac_21	cteraceae	0.01248
Primer16	Bacteria;Proteobacteria;Deltaproteobacteria;Desulfobacterales;Desulfobac	
S_Bac_28	teraceae	0.01218
Primer16	Bacteria;Proteobacteria;Deltaproteobacteria;Desulfobacterales;Desulfobul	
S_Bac_29	baceae	0.00744
Primer16	Bacteria;Proteobacteria;Deltaproteobacteria;Sh765B-TzT-29;uncultured	
S_Bac_31	delta proteobacterium	0.01246
Primer16	Bacteria;Proteobacteria;Epsilonproteobacteria;Campylobacterales;Helicob	
S_Bac_32	acteraceae	0.00372
Primer16	Bacteria;Proteobacteria;Gammaproteobacteria;BD7-8 marine	
S_Bac_35	group;uncultured bacterium	0.02819
Primer16	Bacteria;Proteobacteria;Gammaproteobacteria;E01-9C-26 marine	
S_Bac_37	group;uncultured bacterium HERMI11	0.00922
Primer16	Bacteria;Proteobacteria;Gammaproteobacteria;KI89A clade;uncultured	
S_Bac_38	gamma proteobacterium	0.11585
Primer16	Bacteria;Proteobacteria;Gammaproteobacteria;Oceanospirillales;OM182	
S_Bac_39	clade	0.01344
Primer16	Bacteria;Proteobacteria;Gammaproteobacteria;Oceanospirillales;Oceanosp	
S_Bac_40	irillaceae	0.04369
Primer16	Bacteria;Proteobacteria;Gammaproteobacteria;Oceanospirillales;SS1-B-0	0.00422

S_Bac_41	6-26	
Primer16	Bacteria;Proteobacteria;Gammaproteobacteria;Order Incertae	
S_Bac_42	Sedis;Family Incertae Sedis	0.04639
Primer16	Bacteria;Proteobacteria;Gammaproteobacteria;Xanthomonadales;Sinobact	
S_Bac_46	eraceae	0.02341
Primer16		
S_Bac_48	Bacteria;Verrucomicrobia;Verrucomicrobiae;Verrucomicrobiales;DEV007	0.00691

Table 3 lists the OTU set contents that correlated with Cs cluster elements, including radiocesium, and the relative intensity of each OTU in the biofilm community. The most abundant taxa in this OTU set were *Hexacorallia* and *Oligochaete* among the eukaryotes. For bacteria, high relative intensities of *Bacteroidetes*, *Rhodobacteraceae*, and *Gammaproteobacteria* were observed. Although a primer set that did not target Archaea was used, archeal sequences were obtained in this work by sequencing amplicons generated using the 16S ribosomal RNA primer set. An uncultured *Crenarcheota* in marine group I was observed to be one of the dominant OTUs with a correlation with Cs cluster elements. Previously, *Alpha-* and *Gamma-proteobacteria* have been obtained from biofilms on the surface of nuclear fuel pools (Sarró et al., 2005). According to Sarro et al. (Sarró et al., 2005), biofilms obtained from nuclear fuel pools accumulate ^{60}Co. In our study, cobalt accumulation in the week 1 sample was suggested by the PCA data (Fig. 2B upper panel and Table S1) despite a lack of ^{60}Co signal during gamma-ray spectroscopy. Microbial community retrieved from nuclear fuel pools have been described previously as capable of accumulating both ^{60}Co and ^{137}Cs (Tišáková et al., 2012). Our results suggest that the biofilm sampled in week 1 in our study presents similar characteristics to the microbes described by Sarro et al. and Tisakova et al. in the above-mentioned previous studies.

271

272 Conclusions

273 In this study, we found that biofilms retain a relatively high amount of radioactive cesium in
274 their microbial communities even after more than half a year from the release of radioactive
275 elements into oceans due to nuclear power plant accidents. Our statistical analysis also
276 indicated that different community structures of biofilms show different affinities for
277 radiocesium. Our results suggested biofilms as a point of entry for radioactive elements into
278 the eco-system owing to long-term retention of radiocesium in the biofilm communities.
279 In the future, further research on the accumulation and retention of radioactive elements by
280 marine biofilm communities needs to be undertaken to obtain information that can be used
281 for developing ways to eliminate radioactive contamination and for monitoring of
282 environmental pollution by radiocesium.

283

284

285 Acknowledgements

286 This work was supported by grants for the RIKEN Incentive Research Project (FY2011)
287 “Emergency monitoring for possible cycling of radio active compounds via oceanic food web”
288 awarded to SM and HO and a MEXT Grant-in-Aid for Scientific Research on Innovative
289 Areas (No. 23117003) awarded to SM and KK. We also wish to thank the Iwaki City Fishery
290 Association for permitting the sampling for our study and for providing the fishing vessel
291 Shyo-ei-maru and supporting crew belonging to the abalone section of the Iwaki Fishery
292 Association for our study. We are also grateful to Toshiyuki Suzuki for overseeing and

293 ensuring the diving safety of SM. The authors also wish to acknowledge the profound
294 academic comments and proofreading provided by R. Craig Everroad and Diogo M. O.
295 Ogawa.

296

297

298 References

299 Agostinelli, S., Allison, J., Amako, K., Apostolakis, J., Araujo, H., Arce, P., Asai, M., Axen, D.,
300 Banerjee, S., Barrand, G., et al. (2003). Geant4—a simulation toolkit. *Nuclear*
301 *Instruments and Methods in Physics Research Section A: Accelerators, Spectrometers,*
302 *Detectors and Associated Equipment* 506, 250–303.

303 Allison, J., Amako, K. and Apostolakis, J. (2006). IEEE Xplore Abstract - Geant4
304 developments and applications. *Nuclear Science* 53, 270–278.

305 Caporaso, J. G., Kuczynski, J., Stombaugh, J., Bittinger, K., Bushman, F. D., Costello, E. K.,
306 Fierer, N., Peña, A. G., Goodrich, J. K., Gordon, J. I., et al. (2010). QIIME allows
307 analysis of high-throughput community sequencing data. *Nat. Methods* 7, 335–336.

308 Caporaso, J. G., Lauber, C. L., Walters, W. A., Berg-Lyons, D., Huntley, J., Fierer, N.,
309 Owens, S. M., Betley, J., Fraser, L., Bauer, M., et al. (2012). Ultra-high-throughput
310 microbial community analysis on the Illumina HiSeq and MiSeq platforms. *ISME J* 6,
311 1621–1624.

312 Caporaso, J. G., Lauber, C. L., Walters, W. A., Berg-Lyons, D., Lozupone, C. A., Turnbaugh,
313 P. J., Fierer, N. and Knight, R. (2011). Global patterns of 16S rRNA diversity at a depth
314 of millions of sequences per sample. *Proceedings of the National Academy of Sciences*
315 108 Suppl 1, 4516–4522.

316 HABA, H., KANAYA, J., MUKAI, H., KAMBARA, T. and KASE, M. (2012). One-year
317 monitoring of airborne radionuclides in Wako, Japan, after the Fukushima Dai-ichi
318 nuclear power plant accident in 2011. *Geochem. J.* 46, 271–278.

319 Hirayama, H., Namito, Y., Nelson, W. R. and Bielajew, A. F. (2005). The EGS5 code system.

320 Itouga M., Kato Y., Sakakibara H. (2014). Phenotypic plasticity and mineral nutrient
321 uptake of the moss Polytrichum commune Hedw. (Polytrichaceae, Bryophyta) during
322 acclimation to a change in light intensity. *Hikobia* 16, 459–466.

323 Kanda, J. (2012). Long-term Sources:To what extent are marine sediments, coastal
324 groundwater, and rivers a source of ongoing contaminaton? pp. 1–19. Tokyo.

325 Sarró, M. I., García, A. M. and Moreno, D. A. (2005). Biofilm formation in spent nuclear fuel
326 pools and bioremediation of radioactive water. *Int. Microbiol.* 8, 223–230.

327 Stoeck, T., Bass, D., Nebel, M., Christen, R., Jones, M. D. M., Breiner, H.-W. and Richards, T.
328 A. (2010). Multiple marker parallel tag environmental DNA sequencing reveals a highly
329 complex eukaryotic community in marine anoxic water. *Mol Ecol* 19 Suppl 1, 21–31.

330 Team, R. C. (2014). R: A language and environment for statistical computing.
331 *www.R-project.org*.

332 Tišáková, L., Pipíška, M., Godány, A., Horník, M., Vidová, B. and Augustín, J. (2012).
333 Bioaccumulation of 137Cs and 60Co by bacteria isolated from spent nuclear fuel pools. *J*
334 *Radioanal Nucl Chem* 295, 737–748.

335 Wada, T., Nemoto, Y., Shimamura, S., Fujita, T., Mizuno, T., Sohtome, T., Kamiyama, K.,
336 Morita, T. and Igarashi, S. (2013). Effects of the nuclear disaster on marine products in
337 Fukushima. *Journal of Environmental Radioactivity* 124, 246–254.

338 Zhao, X., Valen, E., Parker, B. J. and Sandelin, A. (2011). Systematic clustering of
339 transcription start site landscapes. *PLoS ONE* 6, e23409.

340

341 Figure legends

342 Figure 1

343 Heatmap chart of the elements and radioactivity data from the biofilm samples based on
344 hierarchical clustering analysis (HCA). The heatmap chart was sorted by HCA for both axes
345 (elements axis and sample axis). Boxes indicate clusters of radiocesium (Cs cluster) or
346 lanthanides (Lanth cluster).

347

348 Figure 2

349 Principal component analysis (PCA) results for the sampling sites with microbial consortia

data and element data with radiocesium. Panel A is the PCA score plot among sampling sites. Each dot indicates one sampling site. Panel B indicates the loading plot of the elements data. The upper panel shows the plot of elements that contribute to the PC1-negative and PC2-positive directions (supplementary table 1), indicating that they contribute to separate week 1 samples in the PC1-negative and PC2-positive directions. The lower panel shows the plot of elements that contribute to the PC1-negative and PC2-negative directions (supplementary table 2), indicating that they contribute to separate week 3 samples in the PC1-negative and PC2-negative directions in the PCA score plot. Panel C indicates the loading plot of the microbial consortia data. The upper panel displays the plot of operational taxonomic units (OTUs) that contribute to the PC1-negative and PC2-positive direction (supplementary table 1), indicating that they contribute to separate week 1 samples in the PCA score plot. The lower panel shows the plot of the OTUs that contribute to the PC1-negative and PC2-negative directions (supplementary table 2), indicating that they contribute to separate week 3 samples in the PCA score plot.

Figure 3

Heatmap chart of microbial consortia data for biofilms with HCA.

The heatmap chart has been sorted by HCA for both axes (OTU axis and sample axis). Green and blue dots indicate contributing OTUs for the PC1-negative and PC2-positive directions and the PC1/PC2-negative direction, respectively. The relative intensity value has been scaled and centered in the row direction.

372 Supplementary tables.xlsx

373 Supplementary table 1

374 Supplementary table 2

Fig.1

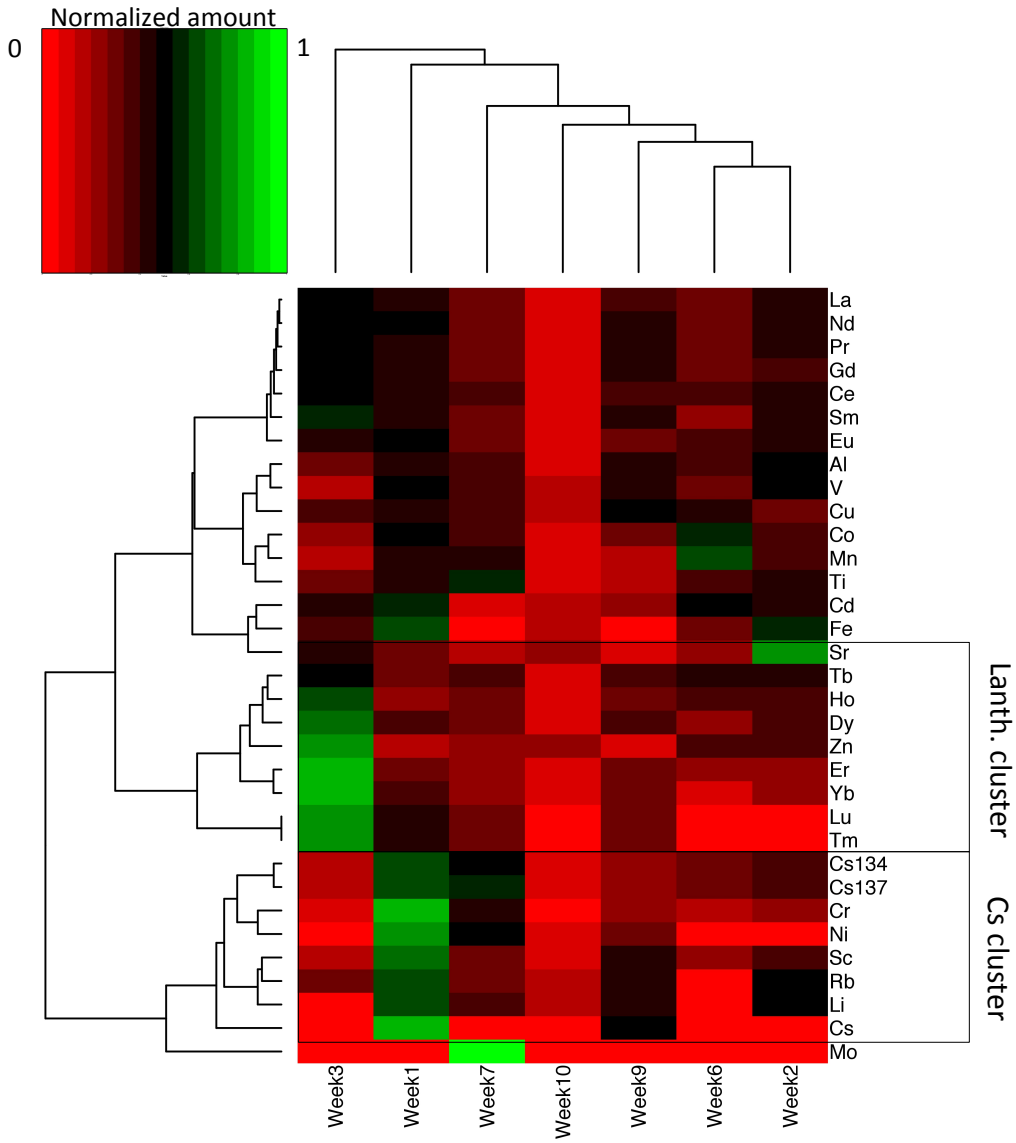

Fig.2

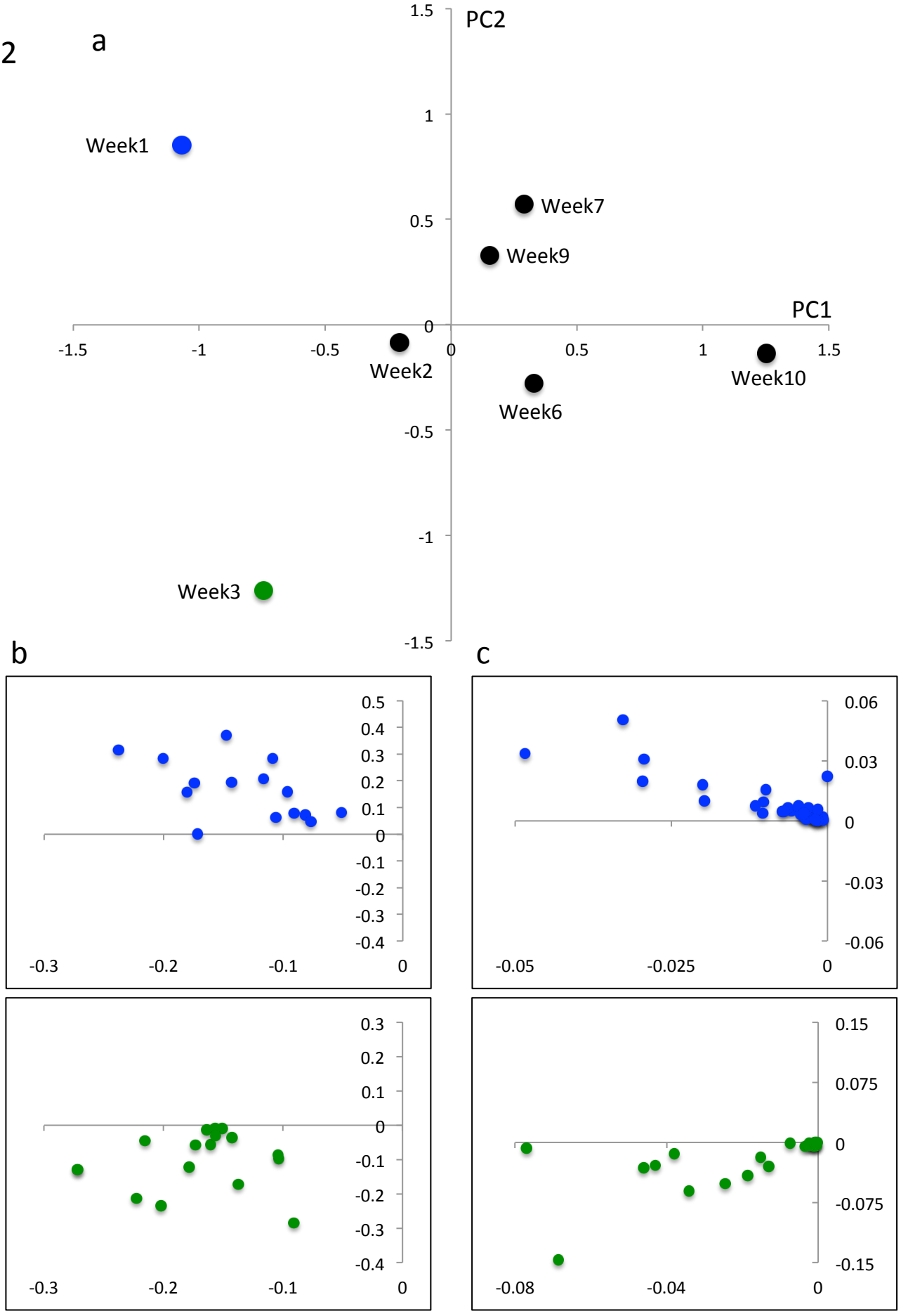

Fig.3